Draft version March 11, 2019
Preprint typeset using LaTeX style emulateapj v. 12/16/11

LYMAN-α IN THE GJ 1132 SYSTEM: STELLAR EMISSION AND PLANETARY ATMOSPHERIC EVOLUTION

William C. Waalkes[1†], Zachory Berta-Thompson[1], Vincent Bourrier[2], David Charbonneau[3], Jonathan Irwin[4], Elisabeth Newton[5], David Ehrenreich[2], Jason Dittmann[5], and Eliza M.-R. Kempton[6,7]

[1]Department of Astrophysical & Planetary Sciences, 391 UCB 2000 Colorado Ave, Boulder, CO 80309, USA, [2]Observatoire Astronomique de l'Université de Genve, 51 chemin des Maillettes, 1290 Versoix, Switzerland, [3]Harvard Astronomy Department, 60 Garden St., MS 46 Cambridge, MA 02138, USA, [4]Smithsonian Astrophysical Observatory, 60 Garden St., Cambridge, MA 02138, USA, [5]MIT, 77 Massachusetts Avenue, Cambridge, MA 02139, USA, [6]Department of Astronomy, University of Maryland, College Park, MD 20742, USA, [7]Department of Physics, Grinnell College, 1116 8th Avenue, Grinnell, IA 50112, USA and
† NSF Fellow

Draft version March 11, 2019

ABSTRACT

GJ 1132b is one of the few known Earth-sized planets, and at 12pc away it is also one of the closest known transiting planets. At ∼19x Earth insolation, this planet is too hot to be habitable but we can use it to learn about the presence and volatile content of rocky planet atmospheres around M dwarf stars. Using Hubble STIS spectra obtained during primary transit, we search for a Lyα transit. If we were to observe a deep Lyα transit, that would indicate the presence of a neutral hydrogen envelope flowing from GJ 1132b. On the other hand, ruling out deep absorption from neutral hydrogen may indicate that this planet does not have a detectable amount of hydrogen loss, is not losing hydrogen, has retained its volatiles, or has lost them very early in the stars life. Our data are consistent with the 1-41% M dwarf UV variability found by Loyd & France (2014), and we do not detect a transit but report a quantitative 2-σ upper limit on the effective cloud radius of 0.36 R_* in the red wing of Lyα, which is the portion of the spectrum we detect after ISM absorption. We also analyze the stellar variability and Lyα spectrum of GJ1132, a slowly-rotating 0.18 solar mass M dwarf with previously uncharacterized UV activity. Understanding the role that UV variability plays in planetary atmospheres and volatile retention is crucial to assess atmospheric evolution and the habitability of cooler rocky planets.

Keywords: Extrasolar Planets, Stellar Spectra

1. INTRODUCTION

The recent discoveries of terrestrial planets orbiting nearby M dwarfs (Gillon et al. 2017; Berta-Thompson et al. 2015; Dittmann et al. 2017; Bonfils et al. 2018; Ment et al. 2018) provide us with the first opportunity to study small terrestrial planets outside our solar system, and observatories such as the Hubble Space Telescope allow us to analyze the atmospheres of these rocky exoplanets. Additionally, it is important that we learn as much as we can about these planets as we prepare for the atmospheric characterization that will be possible with the James Webb Space Telescope (Deming et al. 2009). JWST will provide unique characterization advantages due to its collecting area, spectral range, and array of instruments that allow for both transmission and emission spectroscopy (Beichman et al. 2014).

M dwarfs have been preferred targets for studying Earth-like planets due to their size and temperature which allow for easier detection and characterization of terrestrial exoplanets. However, the variability and high UV-to-bolometric flux ratio of these stars makes habitability a point of contention (e.g., Shields et al. 2016; Tilley et al. 2017). It is currently unknown whether rocky planets around M dwarfs can retain atmospheres and liquid surface water or if UV irradiation and frequent flaring render these planets uninhabitable (e.g., Scalo et al. 2007; Hawley et al. 2014; Luger & Barnes 2014; Bourrier et al. 2017). We must study the UV irradiation environments of these planets, especially given that individual M stars with the same spectral type can exhibit very different UV properties, and a lifetime of UV flux from the host star can have profound impacts on the composition and evolution of their planetary atmospheres.

One aspect of the question of terrestrial planet habitability can be addressed in the context of volatile retention, including the study of water in the planet's atmosphere. One possible pathway of evolution for water on M dwarf terrestrial worlds is the evaporation of surface water and subsequent photolytic destruction of H_2O into H and O species (e.g., Bourrier et al. 2017; Jura 2004). The atmosphere then loses the neutral hydrogen while the oxygen is combined into abiotic O_2/O_3 and/or resorbed into surface sinks (e.g., Wordsworth & Pierrehumbert 2013; Tian & Ida 2015; Luger & Barnes 2014; Shields et al. 2016; Ingersoll & Ingersoll 1969). In this way, large amounts of neutral H can be generated and subsequently lost from planetary atmospheres. Other studies have shown O_2 and O_3 to be unreliable biosignatures because of their ability to be produced abiotically (Tian et al. 2013), so understanding atmospheric photochemistry for terrestrial worlds orbiting M dwarfs is important to our search for life.

1.1. *Prior Work*

Kulow et al. (2014) and Ehrenreich et al. (2015) discovered that Gliese 436b, a warm Neptune orbiting an M dwarf, has a 50% transit depth in the blue-shifted wing of the stellar Lyα line. Lavie et al. (2017) further studied this system to solidify the previous results and verify stellar interactions with the outflowing gas. For planets

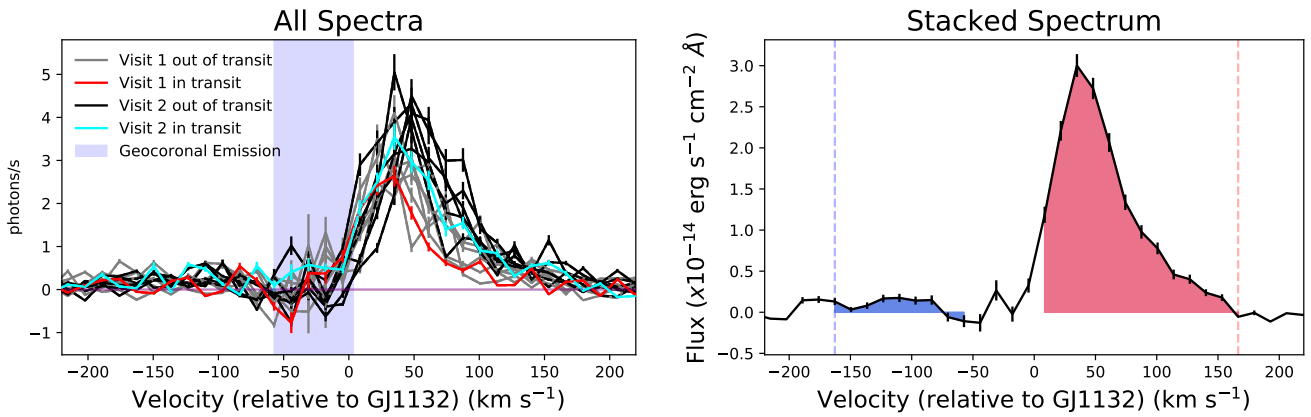

(a) (b)

Figure 1. : All 14 STIS Lyα spectra (a) and the averaged stacked spectrum (b). The shape of the stellar Lyα line is a Voigt profile which has been reshaped by geocoronal emission and ISM absorption by neutral atomic hydrogen and deuterium. The integration regions for summing up the total Lyα flux are the shaded blue and red areas in (b), with a region in the middle that we omit due to the geocoronal emission. It is apparent that the blue-shifted region of the spectrum is at the noise level, and therefore unlikely to give us any viable information. We set the reference velocity for the spectral profiles at 35 km/s, as this is the cited system velocity (Berta-Thompson et al. 2015).

of this size and insolation, atmospheric blowoff can happen as a result of the warming of the upper layers of the atmosphere, which expand and will escape if particles begin reaching escape velocity (e.g., Vidal-Madjar et al. 2003; Lammer et al. 2003; Murray-Clay et al. 2009).

Miguel et al. (2015) find that the source of this outflowing hydrogen is from the H_2-dominated atmosphere of Gl 436b, with reactions fueled by OH^-. Lyα photons from the M dwarf host star dissociate atmospheric H_2O into OH and H, which destroy H_2. HI produced from H_2 and with contributions from the photolyzed H_2O is then the dominant species where $P<5 \times 10^{-5}$ bars.

Modeling of Gl 436b (Bourrier et al. 2015, 2016) demonstrates that the combination of low radiation pressure, low photo-ionization, and charge-exchange with the stellar wind can determine the structure of the outflowing hydrogen, which manifests as a difference in whether the light curve shows a transit in the blue shifted region of Lyα or the red shifted region. Lavie et al. (2017) used new observations to confirm the Bourrier et al. (2016) predictive simulations that this exosphere is shaped by charge-exchange and radiative braking.

As a hydrogen cloud has thus been detected around a warm Neptune, it is important for us to check for similar signals from terrestrial planets. Miguel et al. (2015) also find that photolysis of H_2O also increases CO_2 concentrations. For Earth-like planets orbiting M dwarfs, understanding the photochemical interaction of Lyα photons with water is very important for the evolution and habitability of a planet's atmosphere.

1.2. *GJ 1132b*

GJ 1132b is a small terrestrial planet discovered through the MEarth project (Berta-Thompson et al. 2015). It orbits a 0.181 $M_\odot$ M dwarf located 12 parsecs away with an orbital period of 1.6 days (Dittmann et al. 2017). This is one of the nearest known rocky exoplanets and therefore provides us with a unique opportunity to study terrestrial atmospheric evolution and composition.

While GJ 1132b is too hot to have liquid surface water, it is important to establish whether this planet and others like it retain substantial atmospheres under the intense UV irradiation of their M dwarf host stars, because if they do not, this has implications for the habitability of cooler rocky planets orbiting similar stars. If warm super-Earths such as GJ 1132b cannot regularly retain volatiles such as water in their atmospheres, then we constrain parameter space for atmospheric habitability. However, if even GJ 1132b has retained water vapor, there is additional hope for cooler rocky planets orbiting M dwarfs.

Diamond-Lowe et al. (2018) rule out a low mean-molecular weight atmosphere for this planet by analyzing ground-based transmission spectra at 700-1040 nm. By fitting transmission models for atmospheric pressures of 1-1000 mbar and varying atmospheric composition, they find that all low mean-molecular weight atmospheres are a poor fit to the data, which is better described as a flat transmission spectrum that could be due to a >10x solar metallicity or >10% water abundance. Whether these results imply GJ 1132b has a high mean molecular weight atmosphere or no atmosphere at all remains to be seen. If we detect a Lyα transit then this implies UV photolysis of H_2O into neutral H and O, leading to outflowing neutral H. The oxygen could recombine into O_2 and O_3, leading to a high mean-molecular weight atmosphere, and wholesale oxidation of the surface.

This work serves as the first characterization of whether there is a neutral hydrogen envelope outflowing from GJ 1132b as well as an opportunity to characterize the deepest (longest integration) Lyα spectrum of any quiet M dwarf of this mass.

1.3. *Solar System analogs*

The atmospheric evolution and photochemistry we evaluate here is similar to what we have seen in Mars and Venus. Much of Mars' volatile history has been studied in the context of Lyα observations of a neutral H corona that surrounds present-day Mars. Chaffin et al. (2015) use Lyα observations to constrain Martian neutral H loss coronal structure, similar to what we attempt in this work. Indeed, Mars has historically lost H_2O via photochemical destruction and escape of neutral H, though the solar wind-driven escape mechanisms for Mars are not the same as what we propose for GJ 1132b in this work.

Venus has long been the example for what happens when a terran planet is irradiated beyond the point of habitability, as is more than likely the case with GJ 1132b. Venus experienced a runaway greenhouse effect which caused volatile loss and destruction of H_2O. Kasting & Pollack (1983) study the effects of solar UV radiation on an early Venus atmosphere. They find that within a billion years, Venus could have lost most of a terrestrial ocean of water through hydrodynamic escape of neutral H, after photochemical destruction of H_2O. GJ 1132b has a higher surface gravity than Venus, which would extend this time scale of hydrogen loss. Later in this work, we will estimate the mass loss rate for GJ 1132b based on the stellar Lyα profile.

The rest of the paper will be as follows. In section 2 we describe the methods of analyzing the STIS data, reconstructing the stellar spectrum, and analyzing the light curves. In section 3 we describe the results of fitting for a Lyα transit and reconstructing the spectrum. We discuss the results and their implications in section 4, including estimates of the mass loss rate from this planet's atmosphere. In section 5 we describe what pictures of GJ 1132b's atmosphere we are left with.

2. METHODS

2.1. *Hubble STIS Observations*

To study the potential existence of a neutral hydrogen envelope around this planet, we scheduled 2 transit observations of 7 orbits each with the Space Telescope Imaging Spectrograph (STIS) on the Hubble Space Telescope (HST)[1]. We used the G140M grating with the 52x0.05 slit, collecting data in TIME-TAG mode with the FUV-MAMA photon-counting detector. This resulted in 14 spectra containing the Lyα emission line (1216 Å), which show a broad profile that has been centrally absorbed by neutral ISM atomic hydrogen.

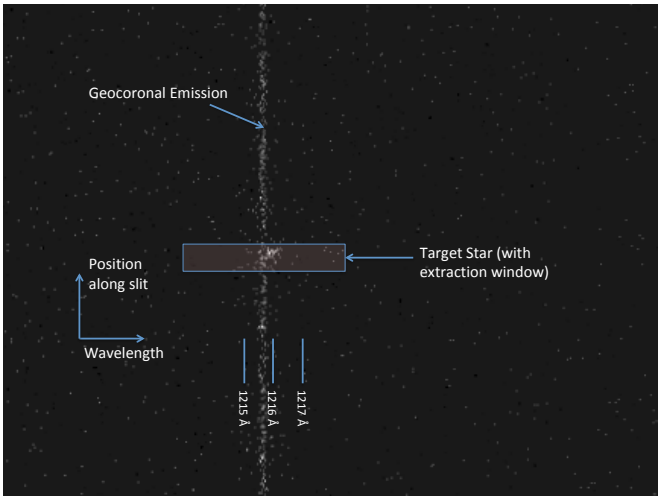

Figure 2. : Image of a STIS x2d spectrum. Geocoronal Lyα is shown as a long vertical line while the GJ 1132 Lyα emission is shown in the center.

We re-extracted the spectra and corrected for geocoronal emission using the `calstis` pipeline (Hodge & Baum 1995). The geocoronal Lyα is emitted from hydrogen around the Earth, which further complicates the signal. We omit data points that fall within the geocoronal emission signal, defining our blue-shifted region to be <-60 km/s and our red-shifted region to be >0 km/s relative to the star. The STIS spectrum extraction involved background subtraction which accounts for geocoronal emission (see Fig. 2), leaving us only with the need to model the stellar emission and ISM absorption. One potential source of variability is where the target star falls on the slit. If it fell directly on the slit, then the observed flux will be more than if the star was partially off the slit. This effect would be more pronounced between visits and within one visit, it would introduce less noise than the STIS breathing effect, which we have demonstrated as being a low source of variability

In order to analyze the light curves with higher temporal resolution, we used the STIS time-tag mode to split each of the 14 2ks exposures into 4 separate 500s sub-exposures. This detector records the arrival time of every single photon, which is what allows us to create sub-exposures in time-tag mode. Each 2D spectrum sub-exposure was then converted into a 1D spectrum. To do this, we first defined an extraction window around the target spectrum (see Fig. 2) and summed up all the flux in that window along the spatial axis. Extraction windows were also defined on either side of the target in order to estimate the background and subtract that from the target window. This results in a noisy line core but eliminates the geocoronal emission signature (Fig. 1a). These steps were all performed with `calstis`.

2.2. *Stellar Spectrum Reconstruction*

With the same spectra used for light curve analysis, we created a single stacked spectrum, representing 29.3ks of integration at Lyα averaged over 14 exposures (Fig. 1b). This stacked spectrum was used with `LyaPy` modeling program (Youngblood et al. 2016) that uses a 9-dimensional MCMC to reconstruct the intrinsic stellar spectrum assuming a Voigt profile. Modeling observed Lyα spectra is tricky because of the neutral ISM hydrogen found between us and GJ 1132. This ISM hydrogen has its own column density, velocity, and line width which creates a characteristic absorption profile within our Lyα emission line.

This model takes 3 ISM absorption parameters (column density, cloud velocity, Doppler parameter) and models the line core absorption while simultaneously modeling the intrinsic emission which would give us the resulting observations. A fixed deuterium-to-hydrogen ratio of 1.56×10^{-5} (Wood et al. 2004) is also applied to account for the deuterium absorption and emission near

[1] Cycle 23 GO proposal 1187, PI: Z Berta-Thompson

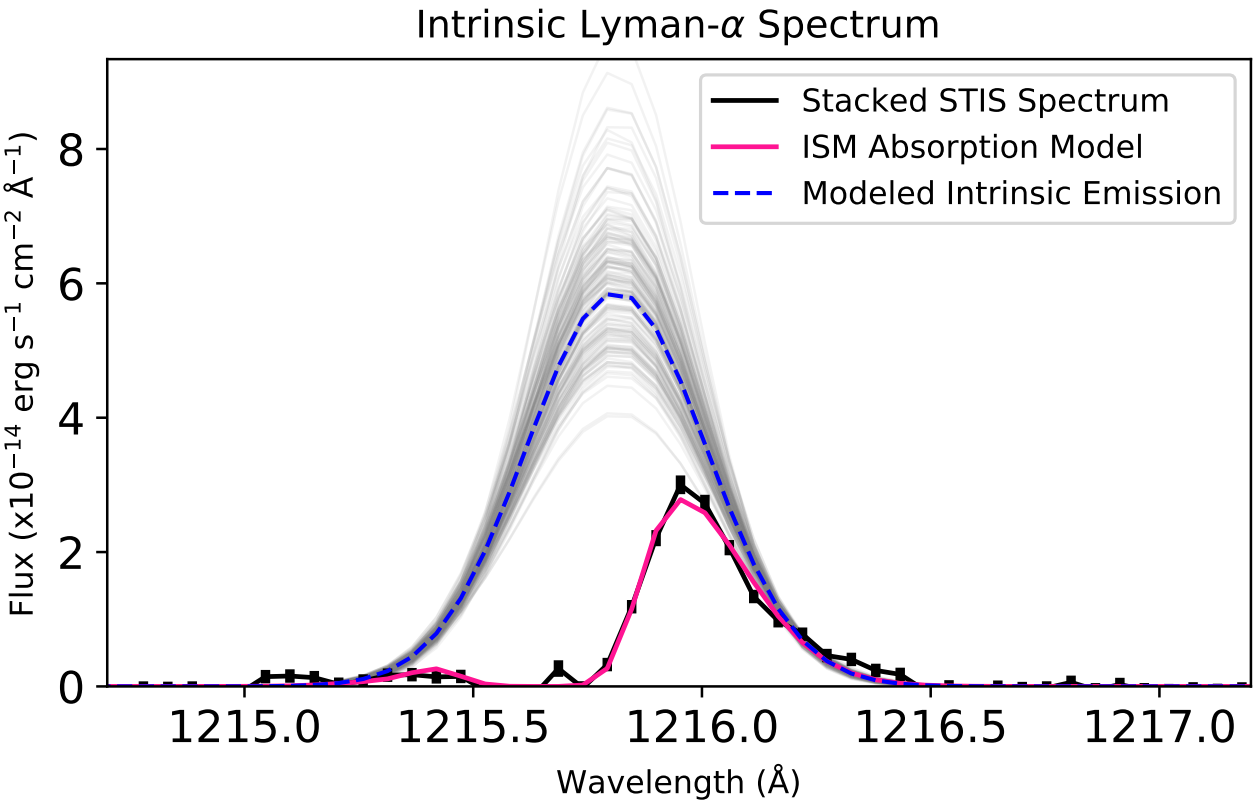

Figure 3. : Intrinsic Lyα profile for GJ 1132b, with 200 random samples in gray. The absorption and intrinsic emission models were modeled with the `Lyapy` software which assumes a Voigt profile for the emission and parameterizes the ISM absorption into velocity, line width, and column density components. Here, the line center is in the system's rest frame.

Lyα. Modeling the ISM parameters required us to approximate the local interstellar medium as a single cloud with uniform velocity, column density, and Doppler parameter. While the local ISM is more complex than this single component and contains two clouds in the line of sight (based on the model described in Redfield & Linsky 2000), our MCMC results strongly favored the velocity of one of these two clouds, so we approximated the ISM parameters to be those of the Local Interstellar Cloud (LIC) (Redfield & Linsky 2000, 2008).

We use uniform priors for the emission amplitude and FWHM, and Gaussian priors for the HI column density, stellar velocity, HI Doppler width, and HI ISM velocity. The HI column density and Doppler width parameter spaces were both truncated in order to prevent the model from exploring physically unrealistic values. For N_{HI}, we restrict the parameter space to 10^{16}-10^{20} cm^{-2}, based on the stellar distance (12.04 pc) and typical n_{HI} values of $0.01 - 0.1$ cm^{-3} (Redfield & Linsky 2000). We limit the Doppler width to 6-18 km/s, based on estimates of the Local Insterstellar Cloud (LIC) ISM temperatures (Redfield & Linsky 2000).

The shape of stellar Lyα emission can have two sources that give rise to a broad and narrow component. The narrow component arises from Alfvén waves while the broad component is likely due to microflares or other explosive events (Wood et al. 1997). Our best fit MCMC model resulted in a single component of emission, with model parameters shown in Table 3 below. While a single component of flux could indicate that the shape of photospheric Lyα is likely due to Alfvén waves rather than the broad component with explosive origins, we cannot rule out the presence of a broad component that may not appear in our low SNR regime.

2.3. *Light Curve Analysis*

The extracted 1D spectra were then split into a blue-shifted regime and red-shifted regime, on either side of the Lyα core (Fig. 1b) so that we could integrate the total blue-shifted and red-shifted flux and create 4 total light curves from the 2 visits (Fig. 5). Each of these light curves was fitted with a `BATMAN` (Kreidberg 2015) light curve using a 2-parameter MCMC with the `emcee` package (Foreman-Mackey et al. 2012). The `BATMAN` models assume that the transiting object is an opaque disk, which is usually appropriate for modeling planetary sizes. However, we are modeling a possible hydrogen exosphere which may or may not be disk-like, and which would have

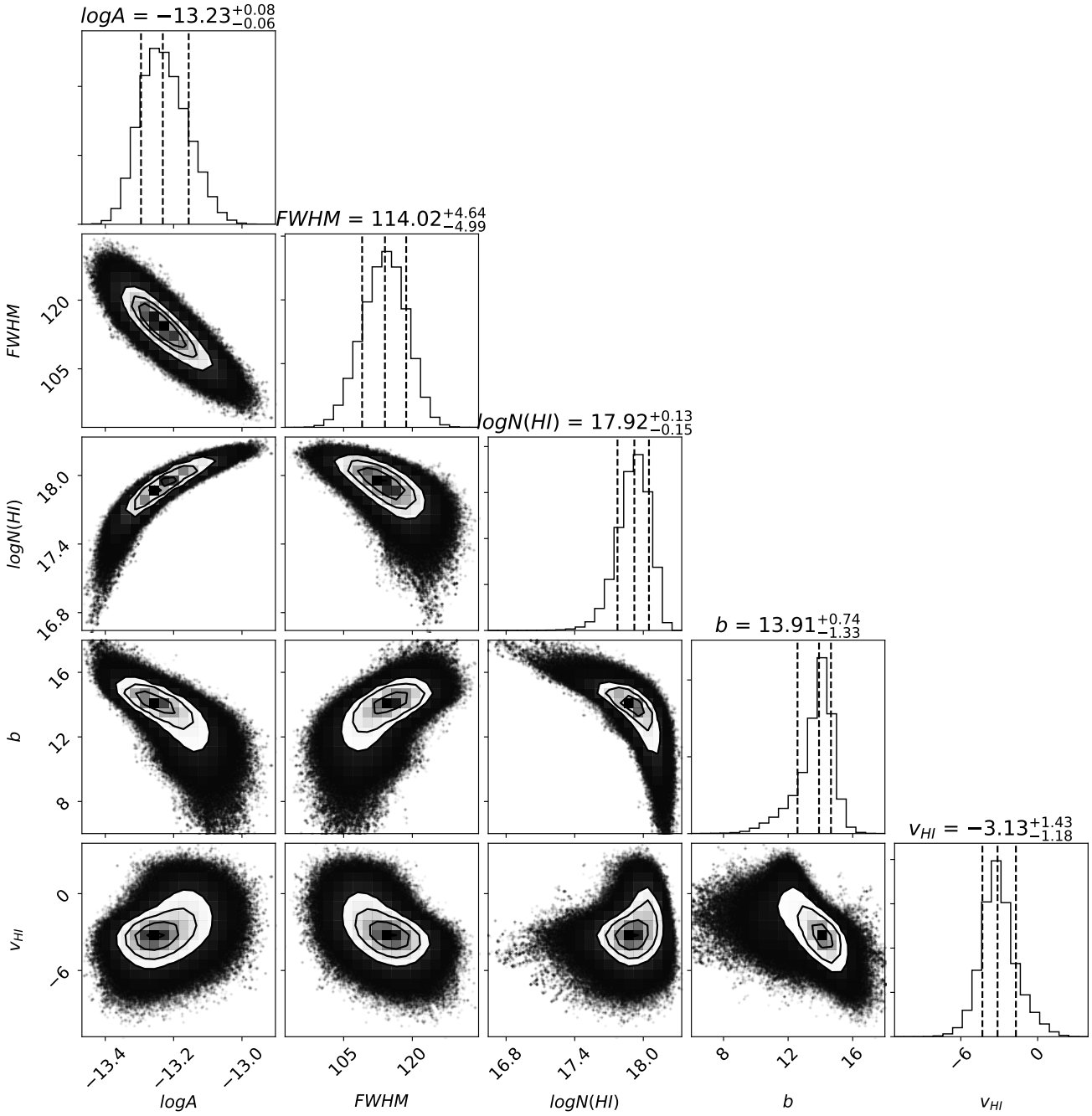

Figure 4. : Corner plot showing the samples used in recreating the intrinsic emission profile. We've omitted the stellar radial velocity samples because the prior was well constrained by independent radial velocity measurements. In this plot, log(A) is the log of the emission amplitude, FWHM is the emission Full Width Half Maximum, log(N(HI)) is the log of the column density of neutral ISM hydrogen, b is the ISM Doppler parameter, and v_{HI} is the ISM cloud velocity.

varying opacity with radius. For this work, we use the `BATMAN` modeling software with the understanding that our results tell us the effective radius of the hydrogen exosphere, with an assumed spherical geometry. We posit that this is appropriate for this first-pass characterization.

We fit for R_p/R_* and the baseline flux using a Poisson likelihood for each visit. We use a Poisson distribution because at Lyα, the STIS detector is receiving very few photons. Our log(likelihood) function is:

$$ln(likelihood) = \sum_i [d_i ln(m_i) - m_i - ln(d_i!)]$$

where d_i is the total (*gross*) number of photons detected

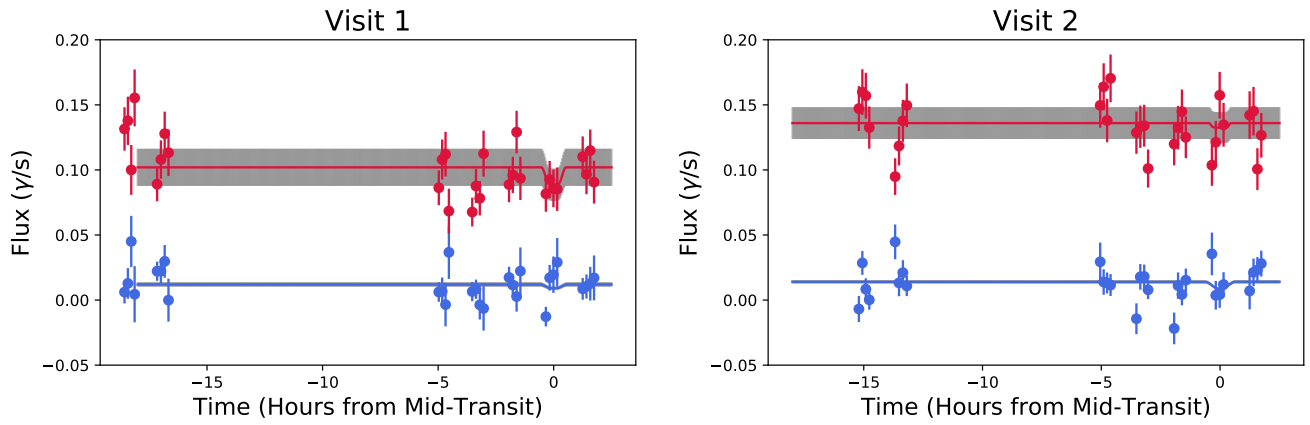

(a) (b)

Figure 5. : Modeled light curves from both visits. The y-axis is in photons/s because the SNR is very low at Lyα. Some data points fall to negative values. This can happen when the data point has effectively no flux and then data reduction processes (such as background subtraction) subtract a slightly higher amount of flux. The gray bars indicate what we calculate as a 15% "stellar variability" fudge factor - acquired by calculating what size of error bars would be necessary to result in a χ^2 value of 1 for our best fit models. The blue wing light curves don't provide much information due to their extremely low flux but we can see from the red wing fits that there is an upper limit on the transit depth.

and m_i is the modeled number of photons detected. The photon model is acquired by taking a `BATMAN` model of in-transit photons and adding the *sky* photons, which is data provided through the `calstis` reduction pipeline. Uniform priors are assumed for both R_p/R_* and the baseline flux.

3. RESULTS

3.1. *Light Curve Modeling*

The light curves for both visits are shown in Figure 5 in units of photons per second as we are at such low flux counts at Lyα. MCMC modeling of these light curves resulted in best fit parameters shown in Table 1. We report no statistically significant transits, but we can use the modeling results to calculate limits on the hydrogen cloud parameters.

3.2. *Stellar Variability*

The red wing of our spectral data show a highly variable stellar Lyα flux over the course of these HST visits and we quantify this variability as a Gaussian uncertainty,

$$\sigma_x^2 = \sigma_{measured}^2 - \sigma_{photometric}^2. \quad (1)$$

Within one 90-minute HST orbit, we see flux variabilities of 5-16% for visit 1 and 7-18% for visit 2. Among one entire 18-hour visit, variability is 20% for visit 1 and 14% for visit 2 while in the 9 months between the two visits, there is a 22% variability. These results are consistent with the 1-41% M dwarf UV variability found by Loyd & France (2014).

3.3. *Spectrum Reconstruction*

Figure 3 shows the best fit emission model with 1-sigma models and a corner plot to display the most crucial modeling parameters, with MCMC results shown in Table 2

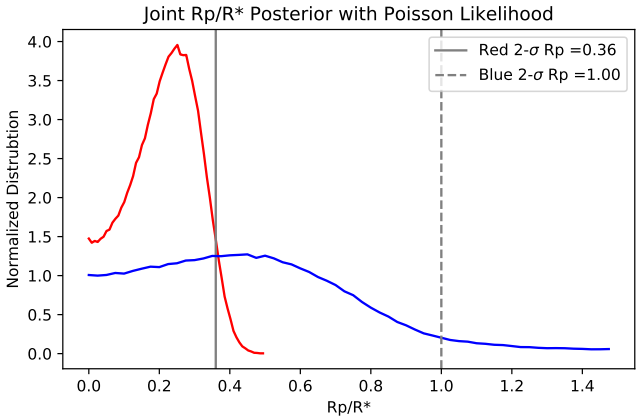

Figure 6. : Joint posterior distribution for the R_p/R_* distributions for both visits. Poisson likelihoods were used due to the low photon count regime of these spectra.

and Figure 4. This result gives us the total Lyα flux for this M dwarf.

The results of the stellar spectrum reconstruction indicate that there is one component of Lyα flux, though that is potentially a result of the low SNR regime of these observations. Additionally, our fit indicates that there is one dominant source of ISM absorption between us and GJ 1132 - a single cloud with velocity -3.1 km/s, HI column density $10^{17.9}$ cm^{-2} and Doppler parameter 13.9 km/s. Our current understanding of the Local Interstellar Cloud (LIC) (Redfield & Linsky 2000, 2008) indicates that there should be 2 clouds, *G* and *Cet* in the line of sight of GJ 1132, but our derived v_{HI} is consistent with the velocity of *G*, which is reported as -2.73 ± 0.94 km/s. We take this to mean that the *G* cloud is the dominant

source of absorption and that we can subsequently reconstruct this spectrum under a single-cloud assumption.

By integrating the reconstructed emission profile, we find a Lyα flux of 2.9x10^{-14} erg/s/cm^2 which gives f[Lyα]/f[bol] = 2.9x10^{-5}, where we have calculated the bolometric luminosity of GJ 1132b as:

$$f_{\rm bol} = \sigma T_{\rm eff}^4 \left(\frac{R_*}{\rm distance}\right)^2, \quad (2)$$

Where values for the T_{eff} and R_* were taken from Bonfils et al. (2018) and the distance to the star is taken from Berta-Thompson et al. (2015). Compared with the Sun which has f[Lyα]/f[bol] = 4.6x10^{-6} (Linsky et al. 2013), we can see that this M dwarf emits a relatively large fraction of its radiation in the ultraviolet.

4. DISCUSSION

With 14 STIS exposures, we have characterized a long-integration Lyα spectrum and furthered our understanding of the intensity of UV flux from this M dwarf, which has many implications for terrestrial atmospheric evolution and long-term habitability. France et al. (2012) find that as much as half of the UV flux of quiescent M dwarfs is emitted at Lyα, having an idea of the total amount of flux at this wavelength serves as a proxy for the total amount of UV flux for this type of star. Despite this relatively high UV flux, further study of terrestrial planet atmospheres is needed to understand the potential habitability of planets orbiting M dwarfs. Our measurement of this Lyα flux provides a useful input for photochemical models of haze, atmospheric escape, and molecular abundances in this planet's atmosphere.

MCMC Results	Visit 1	Visit 2	Joint
R_p/R_* (R)	$0.34^{+0.11}_{-0.15}$	$0.15^{+0.12}_{-0.10}$	$0.22^{+0.09}_{-0.12}$
R_p/R_* (B)	$0.46^{+0.49}_{-0.31}$	$0.58^{+0.38}_{-0.36}$	$0.44^{+0.32}_{-0.18}$
Baseline (γ/s) (R)	$0.102^{+0.003}_{-0.003}$	$0.136^{+0.003}_{-0.004}$	$0.101^{+0.004}_{-0.003}$ $0.136^{+0.003}_{-0.003}$
Baseline (γ/s) (B)	$0.012^{+0.002}_{-0.002}$	$0.014^{+0.002}_{-0.001}$	$0.012^{+0.003}_{-0.002}$ $0.014^{+0.002}_{-0.001}$

Table 1: Light curve fit results for MCMC sampling where Poisson likelihoods were used.

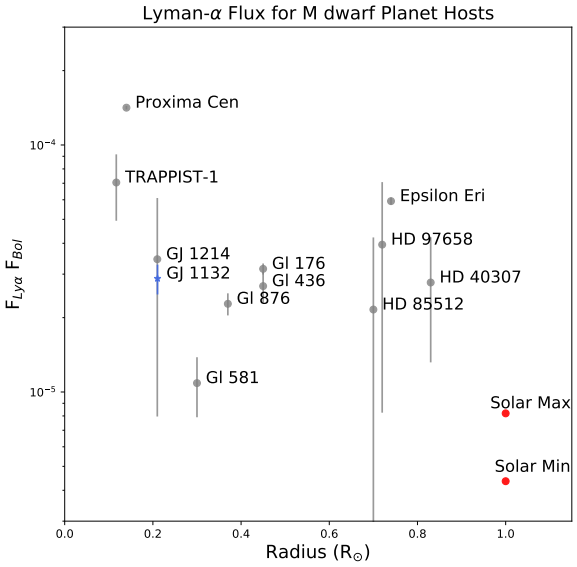

Figure 7. : Comparison of F[Lyα]/F[bol] for GJ 1132 compared with stars in the MUSCLES Treasury Survey (Youngblood et al. 2016, 2017), TRAPPIST-1 (Gillon et al. 2016), as well as the Sun (Linsky et al. 2013). The MUSCLES targets shown here are all M and K dwarfs that are known exoplanet hosts.

Line Velocity [km/s]	$35.23^{+0.99}_{-0.98}$
log(Amplitude) [erg/s/cm^2/Å]	$-13.23^{+0.08}_{-0.06}$
FWHM [km/s]	$114.02^{+4.64}_{-4.99}$
log(HI Column Density) [cm^{-2}]	$17.92^{+0.13}_{-0.15}$
Doppler Parameter (b) [km/s]	$13.91^{+0.74}_{-1.33}$
HI Velocity [km/s]	$-3.13^{+1.43}_{-1.18}$
Total Flux [erg/s/cm^2]	$2.9 \times 10^{-14}{}^{+4\times10^{-15}}_{-3\times10^{-15}}$

Table 2: Intrinsic emission line model parameters taken from MCMC samples, with 1-σ error bars.

From the red-shifted light curves, we can calculate a 2-σ upper limit on the radius of this potential hydrogen cloud outflowing from GJ 1132b. We calculate this upper limit (see Fig. 6) by taking the joint (visit 1 & visit 2) posterior distributions that resulted from MCMC modeling of these light curves and integrating the CDF to the 95% confidence interval and examining the corresponding R_p/R_*. The 2-σ upper limit from the red-shifted Lyα spectra gives us an R_p/R_* of 0.36. This is an upper limit on the effective radius of a hydrogen coma, and the real coma could be much more diffuse and asymmetric.

4.1. *GJ 1132b Atmospheric Loss*

In order to connect our results to an upper limit on the possible mass loss rate of neutral H from this planet's atmosphere, we follow the procedure outlined in Kulow et al. (2014).

Assuming a spherically symmetric outflowing cloud of neutral H, the equation for mass loss is

$$\dot{M}_{HI} = 4\pi r^2 v n_{HI}(r) \quad (3)$$

Where v is the outflowing particle velocity and $n_{HI}(r)$ is the number density of HI at a given radius, r. For this calculation, we will be examining our 2-σ upper limit radius at which the cloud becomes optically thick, where $(R_p/R_*)^2 = \delta = 0.13$. We assume a v range of $10 - 100$ km/s, which is the range of the planet's escape velocity (10 km/s) and the stellar escape velocity (100 km/s).

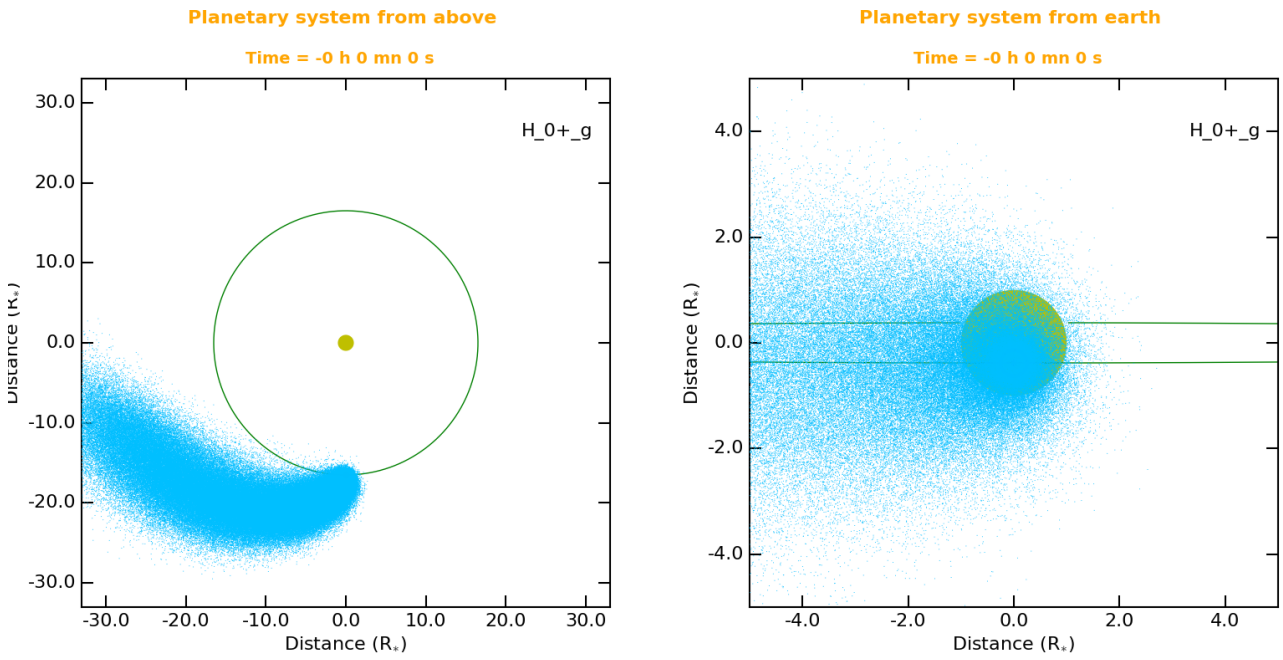

(a) (b)

Figure 8. : Simulations of the GJ1132 system showing the dynamics of a hypothetical outflowing hydrogen cloud. The left panel shows a top-down view of the system, as a hydrogen tail extends in a trailing orbit. The right panel shows the view from an Earth line of sight, at mid-transit.

Kulow et al. (2014) reduce Equation (3) to

$$\dot{M}_{HI} = \frac{2\delta R_* m v}{\sigma_0} \tag{4}$$

with a Lyα absorption cross-section σ_0 defined as

$$\sigma_0 = \frac{\sqrt{\pi} e^2}{m_e c \Delta\nu_D} f \tag{5}$$

where e is the electron charge, m_e is the electron mass, c is the speed of light, f is the particle oscillator strength (taken to be 0.4161 for HI) and $\Delta\nu_D$ is the Doppler width, b/λ_0, where we use 100 km/s for b, as was done in Kulow et al. (2014).

This gives us an upper limit mass loss rate of $\dot{M}_{HI} < 0.86 \times 10^9$ g/s for neutral hydrogen, corresponding to 15.4×10^9 g/s of water decomposition, assuming all escaping neural H comes from H_2O. If this mass loss rate was sustained, GJ 1132b would lose an Earth ocean in approximately 6 Myr. While this is a very rough estimate based on upper limits of what we detect in the data, this mass loss rate indicates that the water content of this world could be lost on time scales shorter than the lifetime of the star.

We can also calculate the energy limited mass loss rate, corresponding to the the ratio of the incoming EUV energy to the work required to lift the particles out of the atmosphere:

$$\dot{M} = \frac{F_{XUV} \pi R_p^2}{G M_p / R_p} = \frac{F_{XUV} \pi R_p^3}{G M_p}. \tag{6}$$

The total F_{XUV} is the flux value at the orbit of GJ 1132b. Using our derived Lyα flux, the `Lyapy` package calculates stellar EUV spectrum and luminosity from 100-1171 Å based on Linsky et al. (2013). From that EUV spectrum, we then calculate the 5-100 Å XUV flux based on relations described in King et al. (2018).

We obtain an energy-limited mass loss rate of 3.0×10^9 g/s estimated from the stellar spectrum reconstruction. This energy-limited escape rate is commensurate with the upper-limit we calculate based on the transit depth and stellar properties in the previous section. If we assume a heating efficiency of 1% (based on similar simulations done in Bourrier et al. 2016), then we arrive at a low neutral hydrogen loss rate of 3.0×10^7 g/s.

4.2. *Simulating HI outflow from GJ 1132b*

Figure 8 shows simulation results for neutral hydrogen outflowing from GJ 1132b from the EVaporating Exoplanet code (`EVE`) (Bourrier et al. 2013, 2016). This code performs a 3D numerical particle simulation given stellar input parameters and atmospheric composition assumptions. These simulations were performed using the Lyα spectrum derived in this work, where the full XUV spectrum has been found as described in the previous section. This spectrum is used directly in `EVE` to calculate the photoionization of the neutral H atoms and calculate theoretical Lyα spectra during the transit of the planet as they would be observed with HST/STIS. In addition, our Lyα spectrum is used to calculate the radiation pressure felt by the escaping neutral hydrogen, which informs the dynamics of the expanding cloud.

EVE simulations were created with the following assumptions: The outflowing neutral hydrogen atoms escape from the Roche lobe altitude ($\sim 5\ R_p$) at a rate of 1×10^7 g/s, modeled as a Maxwellian velocity distribution with upward bulk velocity of 5 km/s and temperature of 7000 K, resulting in a cloud with transit depth ?Rp (Vincent - can you confirm what the expected transit depth of this cloud would be based on your simulations?) (see Salz et al. (2016) for a justification of these parameters). We note that for planets around M dwarfs, the upward velocity may have a strong influence on the extension of the hydrogen coma. The thermosphere is simulated as a 3D grid within the Roche Lobe, defined by a hydrostatic density profile, and the temperature and upward velocity from above. The exosphere is collisionless with its dynamics dominated by radiation pressure.

There might be other processes shaping the exosphere of GJ 1132b (magnetic field, collisions with the stellar wind, the escaping outflow remaining collisional at larger altitudes than the Roche lobe), but for these simulations we take the simplest possible approach based on what we actually know of the system. Finally, we do not include self-shielding effects of HI atoms within the exosphere, as we do not expect the exosphere is dense enough for self-shielding to significantly alter the results.

The integrated Lyα spectrum corresponds with a maximum ratio of stellar radiation pressure to stellar gravity of 0.4, which puts this system in the regime of radiative breaking (Bourrier et al. 2015), which has a slight effect of pushing neutral hydrogen to a larger orbit. However, the gas is not blown away so the size of the hydrogen cloud will increase if we increase the outward particle velocity. Since the exosphere is not accelerated, most of its absorption is close to 0 km/s in the stellar reference frame, with some blue-shifted absorption because atoms in the tail move to a slightly larger orbit than the planet. This indicates that the lack of blue-shifted flux in our observations, due to ISM absorption, is a hindrance to fully understanding the possible hydrogen cloud around this planet. The upper limit cloud size that we quote is based on the observed red-shifted flux in a system which is moving away from us at 35 km/s, so any cloud absorption of flux closer to the line center is outside of the scope of what we can detect.

5. CONCLUSIONS

This work served as a first-pass characterization of the exosphere of GJ 1132b. Until a telescope like LUVOIR (Roberge & Moustakas 2018), these observations will be the deepest possible characterization for Lyα transits of this system. If this planet has a cloud of neutral hydrogen escaping from its upper atmosphere, the effective size of that cloud must be less than 0.36 R_* (7.3 R_p) in the red-shifted wing. In addition, we were able to model the intrinsic stellar spectrum and learn more about the Lyman$-\alpha$ contribution to M dwarf UV flux.

This Lyα transit's upper limit R_p/R_* implies a maximum hydrogen escape rate of $0.08 - 0.86 \times 10^9$ g/s. If this is the case, GJ 1132b loses an Earth ocean of water between $6 - 60$ Myr, which does not bode well for the long-term habitability of terrestrial worlds orbiting M dwarfs. Since the mass loss rate scales linearly with F_{XUV}, we estimate that if this planet were in the habitable zone of its star, about 5x further than its current orbit (based on HZ estimates in Shields et al. 2016), the planet would lose an Earth ocean of water in 0.15-1.5 Gyr. However, these values are based on extreme upper limits and the data suggest mass loss rates lower than these values, so further Lyα observations are needed to better constrain this mass loss.

The relative Lyα/Bolometric flux is roughly 1 order of magnitude higher for this M dwarf than it is for the Sun, which has grave implications for photolytic destruction of molecules in planets around M dwarfs of this mass. Even when considering the EUV spectrum of GJ 1132 (calculated with methods described in Youngblood et al. 2016) and the EUV flux of the Sun (Zhitnitsky 2018), we find that GJ 1132 emits 6x as much EUV flux (relative to F_{bol}) as the Sun.

This work leaves us with several possible pictures of the atmosphere of GJ 1132b:

- The real atmospheric loss rates may be comparable to these upper limits, or they may be much less, which leaves us with an open question about the atmosphere and volatile content of GJ 1132b. There could be some loss, but below the detection limit of our instruments.

- If there is a neutral hydrogen envelope around GJ 1132b, then this super-Earth is actively losing water driven by photochemical destruction and hydrodynamic escape of H. The remaining atmosphere will then be rich in oxygen species such as O_2 and the greenhouse gas CO_2.

- GJ 1132b could be Mars-like or Venus-like, having lost its H_2O long ago, with a thick CO_2 and O_2 atmosphere remaining, or no atmosphere at all. We posit that this is the most likely scenario, and thermal emission observations with JWST (Morley et al. 2017) would give further insight to the atmospheric composition of GJ 1132b.

GJ 1132b presents one of our first opportunities to study terrestrial planet atmospheres and their evolution. While future space observatories will allow us to probe longer wavelength atmospheric signatures, these observations are our current best tool for understanding the hydrogen content and possible volatile content loss of this warm rocky exoplanet.

6. ACKNOWLEDGMENTS

This work is based on observations with the NASA/ESA Hubble Space Telescope obtained at the Space Telescope Science Institute, which is operated by the Association of Universities for Research in Astronomy, Incorporated, under NASA contract NAS5-26555, and financially supported through proposal HST-GO-14757 through the same contract. This project has been carried out in part in the frame of the National Centre for Competence in Research PlanetS supported by the Swiss National Science Foundation (SNSF). VB acknowledges the financial support of the SNSF. This project has received funding from the European Research Council (ERC) under the European Union's Horizon 2020 research and innovation programme (project Four Aces;

grant agreement No 724427). This work was also supported by the NSF GRFP, DGE 1650115.

REFERENCES

Beichman, C., Benneke, B., Knutson, H., et al. 2014, Publications of the Astronomical Society of the Pacific, 126, 1134

Berta-Thompson, Z. K., Irwin, J., Charbonneau, D., et al. 2015, Nature, 527, 204

Bonfils, X., Almenara, J.-M., Cloutier, R., et al. 2018

Bourrier, V., Ehrenreich, D., & des Etangs, A. L. 2015, 65, 1

Bourrier, V., Ehrenreich, D., King, G., et al. 2016

Bourrier, V., Lecavelier des Etangs, A., Dupuy, H., et al. 2013, Astronomy & Astrophysics, 551, A63

Bourrier, V., de Wit, J., Bolmont, E., et al. 2017, The Astronomical Journal, 154, 121

Chaffin, M. S., Chaufray, J. Y., Deighan, J., et al. 2015, Geophysical Research Letters, 42, 9001

Deming, D., Seager, S., Winn, J., et al. 2009, Publications of the Astronomical Society of the Pacific, 121, 952

Diamond-Lowe, H., Berta-Thompson, Z., Charbonneau, D., & Kempton, E. M. R. 2018, eprint arXiv:1805.07328, arXiv:1805.07328

Dittmann, J. A., Irwin, J. M., Charbonneau, D., et al. 2017, arXiv:1704.05556

Ehrenreich, D., Bourrier, V., Wheatley, P. J., et al. 2015, Nature, 522, 459

Foreman-Mackey, D., Hogg, D. W., Lang, D., & Goodman, J. 2012, arXiv:1202.3665

France, K., Linsky, J. L., Tian, F., Froning, C. S., & Roberge, A. 2012, arXiv:arXiv:1204.1976v1

Gillon, M., Jehin, E., Lederer, S. M., et al. 2016, arXiv:1605.07211

Gillon, M., Triaud, A. H. M. J., Demory, B.-O., et al. 2017, Nature, 542, 456

Hawley, S. L., Davenport, J. R. A., Kowalski, A. F., et al. 2014, The Astrophysical Journal, 797, 121

Hodge, P., & Baum, S. 1995, STIS Instrument Science Report 95-007, 14 pages

Ingersoll, A. P., & Ingersoll, A. P. 1969, Journal of the Atmospheric Sciences, 26, 1191

Jura, M. 2004, The Astrophysical Journal, 605, L65

Kasting, J. F., & Pollack, J. B. 1983, Icarus, 53, 479

King, P. K., Fissel, L. M., Chen, C.-Y., & Li, Z.-Y. 2018, Monthly Notices of the Royal Astronomical Society, 474, 5122

Kreidberg, L. 2015, Publications of the Astronomical Society of the Pacific, 127, 1161

Kulow, J. R., France, K., Linsky, J., & Loyd, R. O. P. 2014, arXiv:arXiv:1403.6834v1

Lammer, H., Selsis, F., Ribas, I., et al. 2003, The Astrophysical Journal, 598, L121

Lavie, B., Ehrenreich, D., Bourrier, V., et al. 2017, Astronomy & Astrophysics, 605, L7

Linsky, J. L., Fontenla, J., & France, K. 2013, The Astrophysical Journal, 780, 61

Loyd, R. O. P., & France, K. 2014, The Astrophysical Journal Supplement Series, 211, 9

Luger, R., & Barnes, R. 2014, EXTREME WATER LOSS AND ABIOTIC O 2 BUILDUP ON PLANETS THROUGHOUT THE HABITABLE ZONES OF M DWARFS, Tech. rep., arXiv:arXiv:1411.7412v2

Ment, K., Dittmann, J. A., Astudillo-Defru, N., et al. 2018, A second planet with an Earth-like composition orbiting the nearby M dwarf LHS 1140, Tech. rep., arXiv:arXiv:1808.00485v1

Miguel, Y., Kaltenegger, L., Linsky, J. L., & Rugheimer, S. 2015, MNRAS, 446, 345

Morley, C. V., Kreidberg, L., Rustamkulov, Z., Robinson, T., & Fortney, J. J. 2017, arXiv:1708.04239

Murray-Clay, R. A., Chiang, E. I., & Murray, N. 2009, The Astrophysical Journal, 693, 23

Redfield, S., & Linsky, J. L. 2000, The Astrophysical Journal, 534, 825

—. 2008, The Astrophysical Journal, 673, 283

Roberge, A., & Moustakas, L. A. 2018, Nature Astronomy, 2, 605

Salz, M., Czesla, S., Schneider, P. C., & Schmitt, J. H. M. M. 2016, A&A, 586, doi:10.1051/0004-6361/201526109

Scalo, J., Kaltenegger, L., Segura, A., et al. 2007, Astrobiology, 7, 85

Shields, A. L., Ballard, S., & Johnson, J. A. 2016, Physics Reports, 663, 1

Tian, F., France, K., Linsky, J. L., Mauas, P. J. D., & Vieytes, M. C. 2013, arXiv:1310.2590

Tian, F., & Ida, S. 2015, Nature Geoscience, 8, 177

Tilley, M. A., Segura, A., Meadows, V., Hawley, S., & Davenport, J. 2017, Modeling Repeated M-dwarf Flaring at an Earth-like Planet in the Habitable Zone: I. Atmospheric Effects for an Unmagnetized Planet Running Title: M DWARF FLARES ON HZ EARTH-LIKE PLANET, Tech. rep., arXiv:arXiv:1711.08484v1

Vidal-Madjar, A., des Etangs, A. L., Désert, J.-M., et al. 2003, Nature, 422, 143

Wood, B. E., Linsky, J. L., & Ayres, T. R. 1997, The Astrophysical Journal, 478, 745

Wood, B. E., Linsky, J. L., Hebrard, G., et al. 2004, The Astrophysical Journal, 609, 838

Wordsworth, R. D., & Pierrehumbert, R. T. 2013, The Astrophysical Journal, 778, 154

Youngblood, A., France, K., Loyd, R. O. P., et al. 2016, arXiv:1604.01032

—. 2017, The Astrophysical Journal, 843, 31

Zhitnitsky, A. 2018, Solar Flares and the Axion Quark Nugget Dark Matter Model, Tech. rep., arXiv:arXiv:1801.01509v3